iMAIL

LETTERS TO THE EDITOR

Superficial Calcium Fracture After PCI as Assessed by OCT

Heavily calcified lesions in coronary arteries have been known to cause stent underexpansion, which increases the risk of in-stent restenosis [1,2]. Plaque modification before stent implantation is considered to be the key for treatment of calcified lesions [3]. We hypothesized that calcium fracture by percutaneous coronary intervention (PCI) might be associated with adequate stent expansion and favorable late outcome.

From the coronary catheterization registry of Wakayama Medical University between February 1, 2010 and August 31, 2013, we retrospectively selected 61 patients with chronic stable angina who had a heavily calcified culprit lesion on coronary angiography. The heavily calcified lesion on coronary angiography was identified by radiopacities noted without cardiac motion before contrast injection, generally
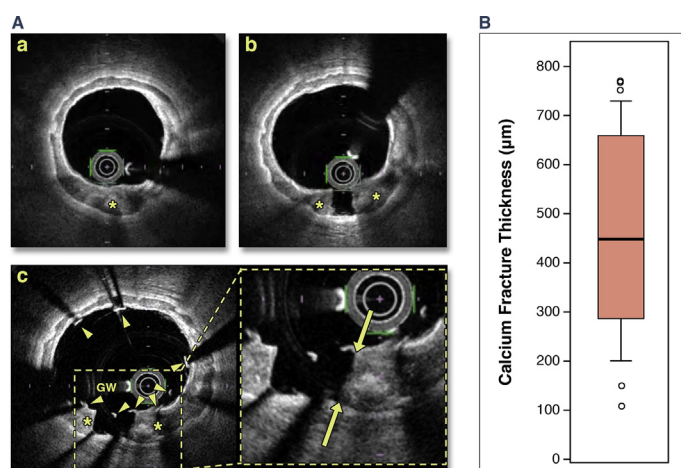

FIGURE 1 Representative OCT Images of Calcium Fracture and Analyzed Data

(A) Optical coherence tomography (OCT) (LUNAWAVE, Terumo, Tokyo, Japan) before percutaneous coronary intervention (PCI) (a) showed entire circumferential calcium. OCT after balloon angioplasty (b) and after PCI (c) demonstrated calcium fracture (6 o'clock). Thickness of the calcium fracture was 710 μm (arrows). **Arrowhead** = stent strut; **asterisk** = calcium; GW = guidewire. (B) The distribution of calcium fracture thickness measured by OCT. Median = 450 μm; lower quartile = 300 μm; upper quartile = 660 μm; minimum = 110 μm; maximum = 770 μm.

compromising both sides of the arterial lumen [4]. Everolimus-eluting stent was used for PCI. PCI procedures including stent size, pre- and post-dilation, and inflation pressure were determined by each physician. Optical coherence tomography (OCT) was performed before and immediately after PCI. Maximal calcium thickness, maximal calcium arc, and maximal calcium length were measured on each candidate frame selected by visual screening in the OCT images before PCI. Calcium fracture and stent expansion were assessed in the OCT images immediately after PCI. Calcium fracture was characterized by a gap of calcium and direct exposure of calcium to the lumen at the gap (**Figure 1A**). The calcium fracture thickness was measured at the edge of the fracture. The minimal stent area was measured on a candidate frame selected by visual screening. Stent expansion index was calculated as the minimal stent area divided by the average of the proximal and distal reference lumen area. Scheduled follow-up angiography was conducted 10 months after PCI.

Calcium fracture was seen in 29 patients (48%) by OCT. Baseline clinical characteristics, angiographic findings before PCI, stent profiles, maximal balloon diameter, and maximal inflation pressure were not different between the groups with and without calcium fracture. The frequency of cutting balloon angioplasty or rotational atherectomy before stent implantation was significantly higher in the group with calcium fracture compared with the group without calcium fracture (24% vs. 3%; p = 0.022). Percent diameter stenosis immediately after PCI was significantly smaller in the group with calcium fracture compared with the group without calcium fracture (5 ± 4% vs. 8 ± 6%; p = 0.027).

OCT-measured maximal calcium thickness, maximal calcium arc, and maximal calcium length were not different between the groups with and without calcium fracture. The median calcium fracture thickness was 450 μm (interquartile range: 300 to 660 μm). The maximal calcium fracture thickness was 770 μm (**Figure 1B**). The minimal stent area was significantly greater in the group with calcium fracture compared with the group without calcium fracture (5.02 ± 1.43 mm^2 vs. 4.33 ± 1.22 mm^2; p = 0.047). Stent expansion index was significantly greater in the group with calcium fracture compared with the group without calcium fracture (0.88 ± 0.17 vs. 0.78 ± 0.18; p = 0.030).

There was no difference in the frequency of procedure-related or in-hospital complications in the groups with and without calcium fracture. The

follow-up angiography at 10 months after PCI was performed in all patients, and percent diameter stenosis was significantly smaller in the group with calcium fracture compared with the group without calcium fracture ($19 \pm 27\%$ vs. $38 \pm 38\%$; $p = 0.030$). The frequency of binary restenosis (14% vs. 41%; $p = 0.024$) and ischemic-driven target lesion revascularization (7% vs. 28%; $p = 0.046$) were significantly lower in the group with calcium fracture compared with the group without calcium fracture.

OCT offers a unique opportunity to observe plaque modification after PCI in the severe calcified lesion. Coronary calcium fracture by PCI was associated with adequate stent expansion and favorable late outcomes. Our findings support and underline the need for optimal lesion preparation in the treatment of heavily calcified lesions.

Takashi Kubo, MD, PhD*
Kunihiro Shimamura, MD
Yasushi Ino, MD, PhD
Tomoyuki Yamaguchi, MD
Yoshiki Matsuo, MD, PhD
Yasutsugu Shiono, MD
Akira Taruya, MD
Tsuyoshi Nishiguchi, MD
Aiko Shimokado, MD
Ikuko Teraguchi, MD, PhD
Makoto Orii, MD
Takashi Yamano, MD
Takashi Tanimoto, MD, PhD
Hironori Kitabata, MD, PhD
Kumiko Hirata, MD, PhD
Atsushi Tanaka, MD, PhD
Takashi Akasaka, MD, PhD

*Department of Cardiovascular Medicine
Wakayama Medical University
811-1 Kimiidera
Wakayama, 641-8509
Japan
E-mail: takakubo@wakayama-med.ac.jp

REFERENCES

1. Madhavan MV, Tarigopula M, Mintz GS, et al. Coronary artery calcification: pathogenesis and prognostic implications. J Am Coll Cardiol 2014;63:1703–14.

2. Kobayashi Y, Okura H, Kume T, et al. Impact of target lesion coronary calcification on stent expansion. Circ J 2014;78:2209–14.

3. Vaquerizo B, Serra A, Miranda F, et al. Aggressive plaque modification with rotational atherectomy and/or cutting balloon before drug-eluting stent

implantation for the treatment of calcified coronary lesions. J Interv Cardiol 2010;23:240–8.

4. Mintz GS, Popma JJ, Pichard AD, et al. Patterns of calcification in coronary artery disease: a statistical analysis of intravascular ultrasound and coronary angiography in 1155 lesions. Circulation 1995;91:1959–65.

Myocardial Kinetics of a Novel [18F]-Labeled Sympathetic Nerve PET Tracer LMI1195 in the Isolated Perfused Rabbit Heart

A radionuclide tracer approach is a unique assay to monitor the cardiac sympathetic nervous system in patients, and the most widely available tracer is the radiolabeled norepinephrine analogue [123I]-metaiodobenzylguanidine ([123I]-MIBG). A novel 18F-labeled positron emission tomography (PET) tracer, [18F]-LMI1195 (N-[3-bromo-4-(3-[18F]fluoropropoxy)-benzyl]-guanidine), has been developed to overcome the limitations of conventional tracers [1]. [18F]-LMI1195 shares similarities with [123I]-MIBG based on its benzylguanidine structure, but higher sensitivity and specificity and more accurate quantification are expected via the general advantages of PET over single-photon emission computed tomography technology. The high specificity of [18F]-LMI1195 for the norepinephrine transporter was confirmed with a cell-binding assay and in vivo imaging [1,2]. Most recently, a human volunteer study demonstrated promising results with uniform tracer uptake in the ventricular wall and acceptable radiation doses [3].

We aimed to evaluate further tracer kinetics at the nerve terminal. First-pass tracer extraction fraction (EF) and washout were measured in isolated rabbit hearts (New Zealand White) to avoid systemic recirculation and metabolism of the tracer.

The EF was determined at different flow values (n = 19). Additionally, the influence of desipramine hydrochloride (40 nM) added into the buffer (n = 5) and reserpine–pre-treated hearts (n = 5) were tested. Reserpine pre-treatment was performed with intravenous injection of reserpine (2 mg/kg) 3 h before the study.

A second protocol was designed to measure tracer washout. Hearts were perfused with [18F]-LMI1195 added to the buffer for 10 min (incubation phase) followed by 25 min of perfusion without tracer (washout phase). The tracer washout was examined by control Krebs-Henseleit bicarbonate buffer (n = 9), and desipramine was added (desipramine-chase; n = 5), with washout with electrical field stimulation (5 Hz, 5 V, 1 min × 5 times at the washout phase; n = 7).